Article

SOURCE DATA | TRANSPARENT PROCESS

EMBO reports

The paracaspase MALT1 mediates CARD14-induced signaling in keratinocytes

Inna S Afonina[1,2], Elien Van Nuffel[1,2], Griet Baudelet[1,2], Yasmine Driege[1,2], Marja Kreike[1,2], Jens Staal[1,2] & Rudi Beyaert[1,2,*]

Abstract

Mutations in *CARD14* have recently been linked to psoriasis susceptibility. CARD14 is an epidermal regulator of NF-κB activation. However, the ability of CARD14 to activate other signaling pathways as well as the biochemical mechanisms that mediate and regulate its function remain to be determined. Here, we report that in addition to NF-κB signaling, CARD14 activates p38 and JNK MAP kinase pathways, all of which are dependent on the paracaspase MALT1. Mechanistically, we demonstrate that CARD14 physically interacts with paracaspase MALT1 and activates MALT1 proteolytic activity and inflammatory gene expression, which are enhanced by psoriasis-associated CARD14 mutations. Moreover, we show that MALT1 deficiency or pharmacological inhibition of MALT1 catalytic activity inhibits pathogenic mutant CARD14-induced cytokine and chemokine expression in human primary keratinocytes. Collectively, our findings demonstrate a novel role for MALT1 in CARD14-induced signaling and indicate MALT1 as a valuable therapeutic target in psoriasis.

Keywords CARD14 signaling pathway; inflammation; MALT1; proteolytic activity; psoriasis

Subject Categories Immunology; Signal Transduction

DOI 10.15252/embr.201642109 | Received 26 January 2016 | Revised 29 March 2016 | Accepted 1 April 2016 | Published online 25 April 2016

EMBO Reports (2016) 17: 914–927

Introduction

Psoriasis is a poorly understood autoimmune disease that affects skin and other organs and is characterized by skin reddening, keratinocyte hyperproliferation, increased inflammatory cytokine and chemokine expression, and infiltration of lesional plaques by T cells and dendritic cells [1]. Several studies have highlighted the importance of genetic factors in the development of psoriasis, but the exact underlying molecular mechanisms are still inadequately defined. It is now generally believed that psoriasis is largely driven by T-cell-mediated immune responses targeting keratinocytes; however, intrinsic alterations in epidermal cells also play a role in disease expression. In particular, keratinocytes may be important in initiating, sustaining, and amplifying the inflammatory response by expressing molecules involved in T-cell recruitment, retention, and activation [2].

Recently, several mutations in *CARD14* (also known as CARMA2 or Bimp2) were identified in both familial and nonfamilial cases of psoriasis, pinpointing *CARD14* as the susceptibility gene of the elusive psoriasis susceptibility locus 2 (PSORS2) in chromosomal region 17q25 [3–6]. Human CARD14 is a 1,004 amino acid long protein that is characterized by a C-terminal membrane-associated guanylate kinase (MAGUK) domain, which is a structural module composed of a PDZ, SH3, and guanylate kinase-like (GUK) domain. At the N-terminus, CARD14 possesses a caspase activation and recruitment domain (CARD), followed by a coiled-coil domain. CARD14 shares a similar domain structure with CARD11 (CARMA1) and CARD10 (CARMA3) proteins, which function as molecular scaffolds in NF-κB signaling induced by antigen receptors and certain G-protein-coupled receptors (GPCRs), respectively [7,8]. More specifically, the CARD domains of CARD10 and CARD11 interact with the CARD domain of BCL10, which itself binds the protease MALT1, also known as paracaspase-1 (PCASP-1) [9]. The resulting CARD10/11–BCL10–MALT1 (CBM) complex then mediates downstream signaling, in which MALT1 has a dual role [7]. On the one hand, MALT1 functions as an essential adaptor for other signaling molecules such as TRAF2 and TRAF6 E3 ubiquitin ligases, which activate downstream protein kinases (TAK1 and IκB kinases) that are involved in NF-κB and MAP kinase signaling. On the other hand, MALT1 is a cysteine protease that cleaves specific signaling proteins and fine-tunes inflammatory signaling by partially understood mechanisms, such as stabilization of mRNA molecules encoding specific cytokines and other inflammatory mediators. Studies in MALT1 knockout and MALT1 protease dead knock-in mice have shown that MALT1 plays a key role in immunity and inflammation by regulating gene expression in lymphocytes and other immune cell types [10]. Moreover, deregulated MALT1 activity has been implicated in certain types of lymphoma [11].

Whereas CARD11 is predominantly expressed in hematopoietic tissues, CARD10 and CARD14 show a much broader expression pattern [4,12]. In the skin, CARD14 strongly localizes to epidermal

1 Unit of Molecular Signal Transduction in Inflammation, Inflammation Research Center, VIB, Ghent, Belgium
2 Department of Biomedical Molecular Biology, Ghent University, Ghent, Belgium
*Corresponding author. Tel: +32 93313770; E-mail: Rudi.Beyaert@irc.vib-ugent.be

keratinocytes. Several CARD14 isoforms have been identified, and most studies focused on a shorter splice variant known as CARD14sh, encoding the first 740 amino acids and lacking the C-terminal SH3 and guanylate kinase-like domains [4,12]. Overexpression of CARD14sh has been shown to activate NF-κB-dependent luciferase reporter gene expression via its N-terminal CARD domain, which was shown to interact with BCL10 [13]. In addition, CARD14sh was reported to interact with TRAF2 and to activate NF-κB in a TRAF2-dependent manner [12]. So far, upstream mechanisms that trigger CARD14-mediated signaling have not yet been identified. Interestingly, overexpression of psoriasis-associated CARD14 mutants in a keratinocyte cell line leads to enhanced NF-κB activation and upregulation of a subset of psoriasis-associated genes, including CCL20, IL-8, and IL-36γ [3].

Because of its key role in the development of psoriasis, a better understanding of the signaling function and mechanism of action of CARD14 is of utmost importance. Here, we have explored the ability of CARD14 to activate multiple signaling pathways, and we investigated the role of paracaspase MALT1 in CARD14-induced signaling and inflammatory gene expression in human keratinocytes.

Results

CARD14 activates NF-κB and p38/JNK MAP kinase signaling

Most of the work published to date on CARD14 signaling was performed with the CARD14sh splice variant [3,4], which lacks the C-terminal SH3 and guanylate kinase-like domains. We therefore first compared the effect of overexpression of full-length CARD14 (further referred as CARD14) and CARD14sh to activate NF-κB-dependent reporter gene expression and IL-8 secretion in HEK293T cells. Both CARD14 and CARD14sh activated expression of the NF-κB reporter gene (Fig 1A) as well as IL-8 (Fig 1B) in a concentration-dependent manner. The slightly less efficient activation of NF-κB and IL-8 induction by CARD14sh relative to CARD14 most likely reflects the somewhat lower expression of CARD14sh, which we noticed in multiple experiments (Fig 1B and C).

Besides NF-κB, also p38 and JNK MAP kinases have been implicated in psoriasis [14,15]. Therefore, we compared the ability of CARD14 and CARD14sh overexpression to activate p38 and JNK MAP kinase signaling in HEK293T cells. p38 and JNK activation is associated with their phosphorylation, which can be revealed via Western blotting of total cell extracts and detection with phospho-p38 and phospho-JNK specific antibodies, respectively. In addition, activation of JNK can also be followed by detecting the phosphorylation and accumulation of c-Jun, whose half-life is increased upon phosphorylation by JNK [16]. CARD14 as well as CARD14sh induced phosphorylation of c-Jun, p38 and JNK, and accumulation of c-Jun (Fig 1C) with similar potency (taking into account slight differences in CARD14 and CARD14sh expression levels; for example, compare lanes 5 and 8 of Fig 1C). We were unable to detect increased ERK phosphorylation upon CARD14 overexpression (Fig EV1). Together, these data clearly demonstrate that CARD14 and CARD14sh not only mediate NF-κB signaling, but also p38 and JNK signaling.

CARD14 physically interacts with MALT1

In antigen receptor-stimulated T and B cells, CARD11 physically interacts with BCL10 and the paracaspase MALT1 to form a so-called CARD11/BCL10/MALT1 (CBM) signalosome that activates downstream signaling [7]. We therefore hypothesized the existence of a similar complex in the case of CARD14. To investigate this, we immunoprecipitated MALT1 from HEK293T cells that were transfected with MALT1, BCL10, and CARD14sh in different combinations and analyzed whether CARD14sh and BCL10 were present in the same complex. CARD14sh co-immunoprecipitated with MALT1, which was further increased upon co-expression of BCL10 (Fig 2A), consistent with BCL10 functioning as an adaptor between CARD14sh and MALT1. Endogenous BCL10 expression most likely explains CARD14sh/MALT1 co-immunoprecipitation without BCL10 co-transfection. Knockdown of endogenous BCL10 also strongly reduced CARD14-induced NF-κB signaling (Fig EV2A). Together, these data suggest the existence of a novel CARD14/BCL10/MALT1 CBM signalosome.

Compared to full-length CARD14, CARD14sh has an incomplete MAGUK signature (lacking the C-terminal SH3 and GUK domains). CARD9, another CARD-containing protein that interacts with the CARD domain of BCL10 and regulates BCL10-MALT1-mediated NF-κB activation in response to dectin-1 stimulation of myeloid cells, lacks the complete MAGUK domain [17,18]. We therefore compared CBM complex formation between CARD9, CARD14sh, CARD14, and constitutively active CARD11(L232LI) [19]. MALT1 co-immunoprecipitated equally well with CARD14sh, CARD14, and CARD11, showing that the absence of the SH3 and GUK domains does not affect CBM complex formation (Fig EV2B). On the other hand, co-immunoprecipitation of CARD9 with MALT1 was much less efficient, especially considering the higher CARD9 expression level. These data suggest unique regulatory mechanisms in the case of CARD9.

MALT1 is indispensable for CARD14-mediated signaling

The above-described physical interaction of CARD14 with MALT1 suggests an important functional role for MALT1 in CARD14 signaling. To investigate this further, we initially analyzed the effect of MALT1 co-expression on CARD14sh-induced p38/JNK and NF-κB signaling in HEK293T cells. Transfection with TRAF6 and CARD11 (L232LI) was used as a positive control. Notably, CARD14sh-induced p38/JNK phosphorylation and c-Jun accumulation were significantly enhanced upon co-expression of MALT1 (Fig 2B). Recently, several psoriasis-associated CARD14 mutations [CARD14 (G117S), CARD14(E138A), and CARD14(E142K)] were shown to potentiate the ability of CARD14sh to activate NF-κB, whereas the pathogenic CARD14(H171N) variant required stimulation with TNF to achieve significant increases in NF-κB activation [3,4]. We here show that the same mutations also enhance NF-κB activation by full-length CARD14, which was even much more pronounced when MALT1 was co-expressed (Fig 2C). To investigate whether pathogenic CARD14 mutations also affect CBM complex formation, we co-transfected HEK293T cells with MALT1 and either CARD14, CARD14(E138A), or CARD14(H171N), and analyzed the ability of the different CARD14 variants to co-immunoprecipitate with MALT1. Interestingly, CARD14(E138A) co-immunoprecipitated more efficiently with MALT1 than CARD14 and CARD14(H171N)

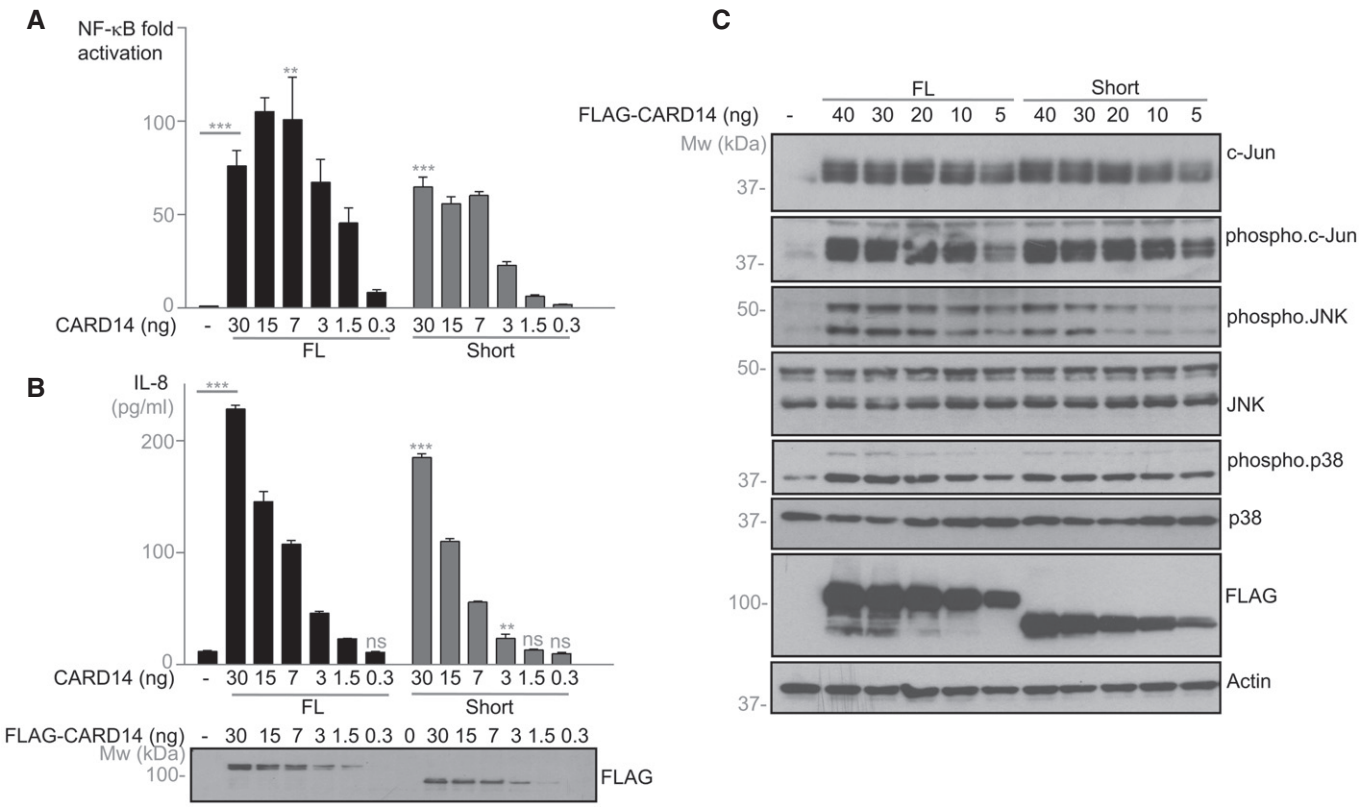

Figure 1. CARD14 and CARD14sh induce NF-κB signaling, IL-8 secretion and JNK/p38 MAP kinase activation.

HEK293T were transfected with NF-κB luciferase reporter plasmid and FLAG-tagged full-length CARD14 (FL) or CARD14sh (short) at the indicated concentrations and analyzed 24 h later.

A NF-κB reporter gene expression.

B IL-8 secretion.

C Immunoblotting for c-Jun, phospho-c-Jun, JNK, phospho-JNK, p38, and phospho-p38 as indicated. Actin was used as a loading control. Data are representative of two independent experiments.

Data information: Values are the mean of triplicates ± SE. *P*-values are compared against empty vector treatment. Significance levels: ns $P > 0.05$, $^{**}P < 0.01$, and $^{***}P < 0.001$ by Student's *t*-test. Unless otherwise indicated, *P*-values are $P < 0.001$ (only shown for the highest CARD14 concentration).

Source data are available online for this figure.

(Fig 2D), which is consistent with the NF-κB promoting activity of this variant (Fig 2C). Together, these results suggest a role for enhanced MALT1 activation in pathogenic CARD14 signaling.

To further investigate whether MALT1 is essential for CARD14-mediated signaling, we generated MALT1-deficient HEK293T cells via TALEN-mediated genome editing and analyzed the ability of CARD14sh to induce NF-κB activation in these cells. CARD11-induced (MALT1-dependent; [7]) and TRAF6-induced (MALT1-independent) NF-κB activations were used as positive and negative controls, respectively. Importantly, overexpression of CARD14sh failed to activate NF-κB in MALT1-deficient cells while reconstitution with wild-type MALT1 restored the ability of CARD14sh to activate NF-κB (Fig 3A). CARD14sh-induced NF-κB activation in the presence of MALT1 was further promoted by BCL10 transfection (Fig 3A), consistent with a role in CBM complex formation as described above. Similar to NF-κB activation, CARD14sh-induced JNK phosphorylation and c-Jun accumulation were completely compromised in the absence of MALT1, which could be rescued upon re-introduction of MALT1 (Fig 3B). Of note, reconstitution of MALT1-deficient cells with a catalytically inactive MALT1(C/A) mutant also restored CARD14sh-induced JNK signaling (Fig 3B), indicating that CARD14sh-induced JNK is strictly dependent on MALT1 scaffold function but does not require MALT1 proteolytic activity.

To extend our observations to a physiologically more relevant cell type, we took advantage of the human keratinocyte HaCaT cell line, which we stably transfected with a doxycycline-inducible full-length CARD14 construct. Doxycycline-induced CARD14 expression increased IL-8 and MCP-1 secretion (Fig 3C). Importantly, siRNA-mediated knockdown of MALT1 expression efficiently inhibited CARD14-induced IL-8 and MCP-1 secretion, while non-targeting siRNA had no effect (Fig 3C). Collectively, these data demonstrate that MALT1 is indispensable for CARD14-induced inflammatory signaling.

Psoriasis-associated CARD14 mutation enhances MALT1 catalytic activity

To investigate whether CARD14 is able to activate MALT1 catalytic activity, we analyzed whether CARD14 overexpression in HEK293T

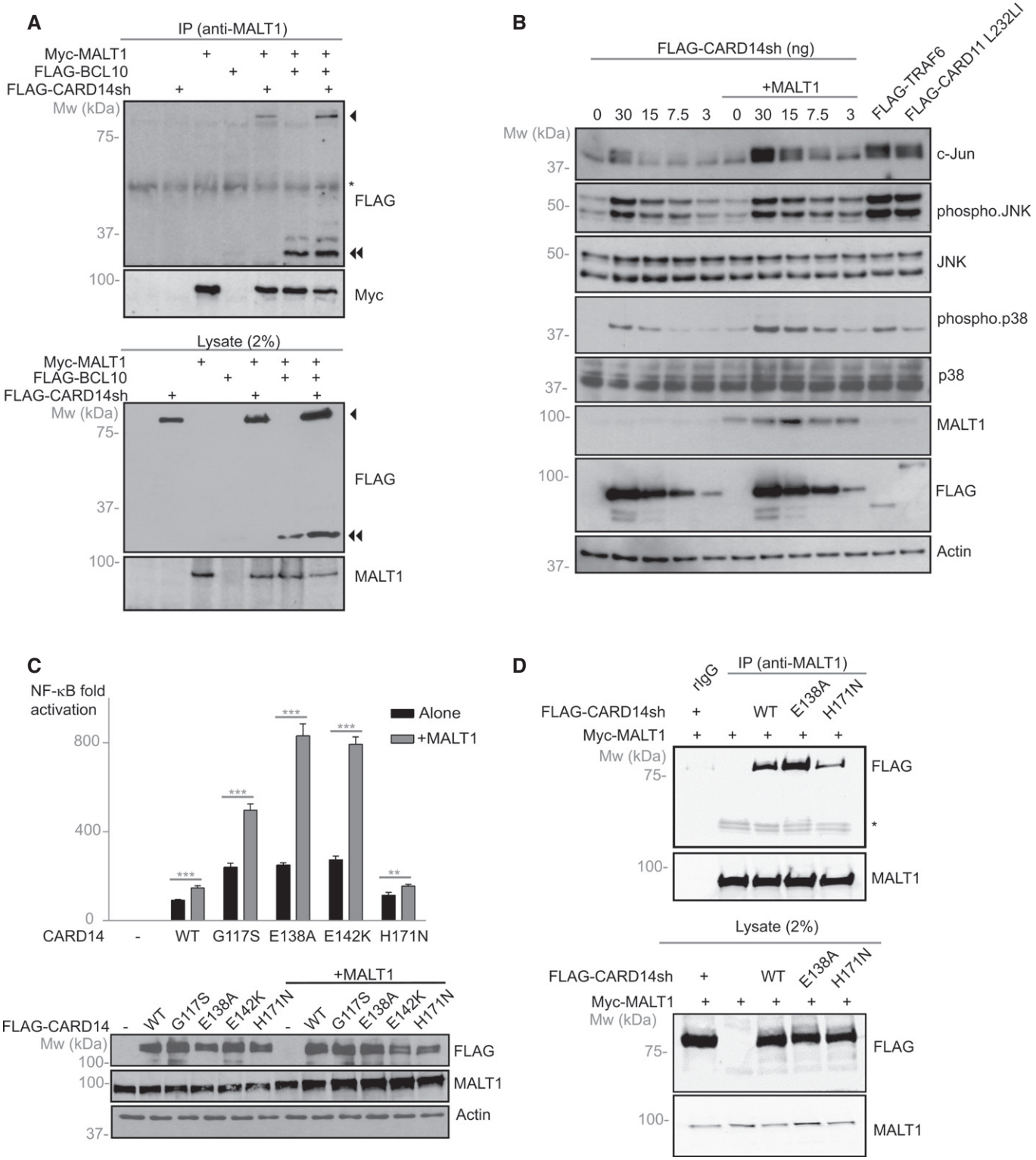

Figure 2.

cells induces the proteolytic processing of endogenously expressed CYLD and A20, which are known MALT1 substrates in antigen receptor-stimulated T cells [20,21]. CARD11(L232LI) overexpression was used as a positive control. CARD14 clearly induced cleavage of endogenous CYLD and A20 in a CARD14 concentration-dependent manner (Fig 4A). CARD14 signaling did not induce the processing of a CYLD(R324A) mutant in which the known MALT1 cleavage site was mutated (Fig 4B). In addition, CARD14 overexpression failed to induce CYLD cleavage in MALT1-deficient HEK293T cells, which was restored by the re-introduction of wild-type but not catalytically

Figure 2. MALT1 interacts with CARD14 and enables CARD14 signaling, which are enhanced by pathogenic CARD14 mutations.

A MALT1 interacts with CARD14sh in a BCL10-dependent manner. HEK293T cells were transfected with FLAG-CARD14sh, Myc-MALT1, and FLAG-BCL10 as indicated. Twenty-four hours later, MALT1 was immunoprecipitated (IP) from cell lysates with anti-MALT1. CARD14sh and BCL10 co-immunoprecipitation with MALT1 was detected by immunoblotting with anti-FLAG. Immunoprecipitated MALT1 was detected by immunoblotting with anti-myc. The closed arrowhead shows the position of CARD14, and the double arrowhead shows the position of BCL10. The asterisk indicates a non-specific band. Total expression levels of transfected proteins are shown by immunoblotting of a fraction of the cell lysates with the indicated antibodies (bottom panel).

B MALT1 co-expression potentiates CARD14sh-induced JNK and p38 MAP kinase activation. HEK293T cells were transfected with the indicated concentrations of FLAG-tagged CARD14sh, with or without MALT1 (30 ng). Transfection with FLAG-TRAF6 and FLAG-CARD11(L232LI) was used as a positive control. c-Jun accumulation, JNK and p38 phosphorylation were analyzed by immunoblotting with the antibodies indicated. Actin was used as a loading control.

C MALT1 co-expression potentiates NF-κB activation by pathogenic CARD14 mutants. HEK293T were transfected with NF-κB reporter plasmid and wild-type (WT) FLAG-CARD14 or the indicated psoriasis-associated CARD14 mutants (15 ng), with or without MALT1 (15 ng). Luciferase activity in cell lysates was measured after 24 h. Values are the mean of triplicates ± SE. Significance levels: $^{**}P < 0.01$ and $^{***}P < 0.001$ by Student's *t*-test. Expression of transfected proteins was verified by Western blotting (bottom panel).

D CARD14(E138A) mutation enhances MALT1 binding. HEK293T cells were transfected with wild-type (WT) FLAG-CARD14sh or the indicated CARD14sh mutants and Myc-MALT1. Twenty-four hours later, MALT1 was immunoprecipitated (IP) from cell lysates with anti-MALT1 and CARD14 co-immunoprecipitation was detected by immunoblotting with anti-FLAG. Immunoprecipitated MALT1 was detected by immunoblotting with anti-MALT1. The asterisk indicates a non-specific band. Immunoprecipitation with a non-relevant antibody (rIgG) was used as a negative control (first lane). Total expression levels of transfected proteins are shown by immunoblotting of total cell lysates (bottom panel). Data are representative of two independent experiments.

Source data are available online for this figure.

inactive MALT1(C/A) (Fig 4C). Together, these data demonstrate that CARD14 activates MALT1 proteolytic activity.

We next compared the ability of wild-type CARD14 and several psoriasis-associated CARD14 mutants to induce CYLD and A20 cleavage in HEK293T cells. Interestingly, the pathogenic mutants CARD14 (G117S), CARD14(E138A), and CARD14(E142K) were all more potent than wild-type CARD14 to induce A20 and CYLD cleavage, whereas the pathogenic CARD14(H171N) variant was equally active (Fig 4D). The different efficiency of several CARD14 variants is consistent with their differential ability to increase NF-κB-dependent reporter gene expression (Fig 2C) and IκBα phosphorylation (Fig 4D). In conclusion, these data demonstrate that psoriasis-associated CARD14 mutations enhance MALT1 proteolytic activity.

MALT1 proteolytic activity in T cells has recently been shown to increase the expression of a subset of cytokines and other inflammatory mediators by proteolytic inactivation of specific mRNA destabilizing proteins [22,23], We therefore analyzed whether pharmacological inhibition of MALT1 proteolytic activity by mepazine had an effect on CARD14-induced gene expression in HaCaT keratinocytes. Mepazine prevented IL-8 and MCP-1 secretion triggered by doxycycline-induced expression of CARD14 in a dose-dependent manner (Fig 4E). In contrast, TNF-induced gene expression was unaffected by mepazine treatment, consistent with MALT1-independent TNF signaling. Collectively, these data demonstrate that CARD14-induced MALT1 proteolytic activity contributes to inflammatory gene expression in keratinocytes.

The psoriasis-associated proteins CYLD, A20, and ABIN-1 negatively regulate CARD14 signaling

The deubiquitinases CYLD and A20, as well as the A20-binding protein ABIN-1 (also known as TNIP-1), are well known because of their anti-inflammatory function and association with several autoimmune diseases including psoriasis [24–27]. They are believed to exert their anti-inflammatory function by dampening multiple signaling pathways such as NF-κB signaling initiated by Toll-like receptors and TNF [28–30]. These activities as well as our observation that CARD14 induces A20 and CYLD cleavage prompted us to investigate whether CYLD or A20 can regulate CARD14-mediated NF-κB signaling. Indeed, CYLD (Fig 5A) as well as A20 overexpression (Fig 5B) significantly inhibited CARD14sh-induced activation of an NF-κB-dependent luciferase reporter gene in a concentration-dependent manner. Similar results were obtained with ABIN-1 (Fig 5C). Recently, the ability of A20 to inhibit TNF-induced NF-κB signaling has been proposed to involve the ubiquitin-binding zinc finger (Znf) 4 and 7 domains of A20, while disruption of its catalytic DUB domain had no effect [31,32]. Similarly, mutation of the DUB domain did not affect the ability of A20 to interfere with CARD14sh-induced NF-κB signaling, whereas mutation of Znf4 and Znf7 completely prevented the inhibitory effect of A20 (Fig 5D). Together, these data demonstrate the potential of CYLD, A20, and ABIN-1 to negatively regulate CARD14 signaling.

Induction of inflammatory gene expression by psoriasis-associated CARD14 mutants in human primary keratinocytes is MALT1-dependent

To investigate the role of MALT1 in pathogenic CARD14-induced inflammatory gene expression, we transfected human primary keratinocytes with the psoriasis-associated mutant CARD14(E138A) and analyzed the secretion of 36 different human cytokines, chemokines, and acute-phase proteins using a multiplex antibody array. CARD14(E138A) expression upregulated multiple cytokines and chemokines, several of which have been associated with psoriasis (GM-CSF, IL-1α, IL-1β, RANTES, Groα, IL-8) [1,33,34] (Fig 6A; a longer exposure of the blot as well as a table showing the location of all tested proteins is shown in Fig EV3A and C). Next, their induction was compared in CARD14(E138A) expressing cells that were transfected with MALT1 siRNA or scrambled siRNA as a negative control. Knockdown of MALT1 strongly reduced CARD14 (E138A)-induced gene expression (Figs 6B and EV3B), demonstrating that psoriasis-associated mutant CARD14(E138A)-induced gene expression in human primary keratinocytes is MALT1-dependent.

We next choose IL-8 as one of the more strongly upregulated genes to analyze the MALT1-dependency of CARD14-induced gene expression in more detail. CARD14(E138A) and CARD14(G117S) were both more potent than wild-type CARD14 in inducing IL-8 (Fig 6C), consistent with their stronger potential to activate NF-κB.

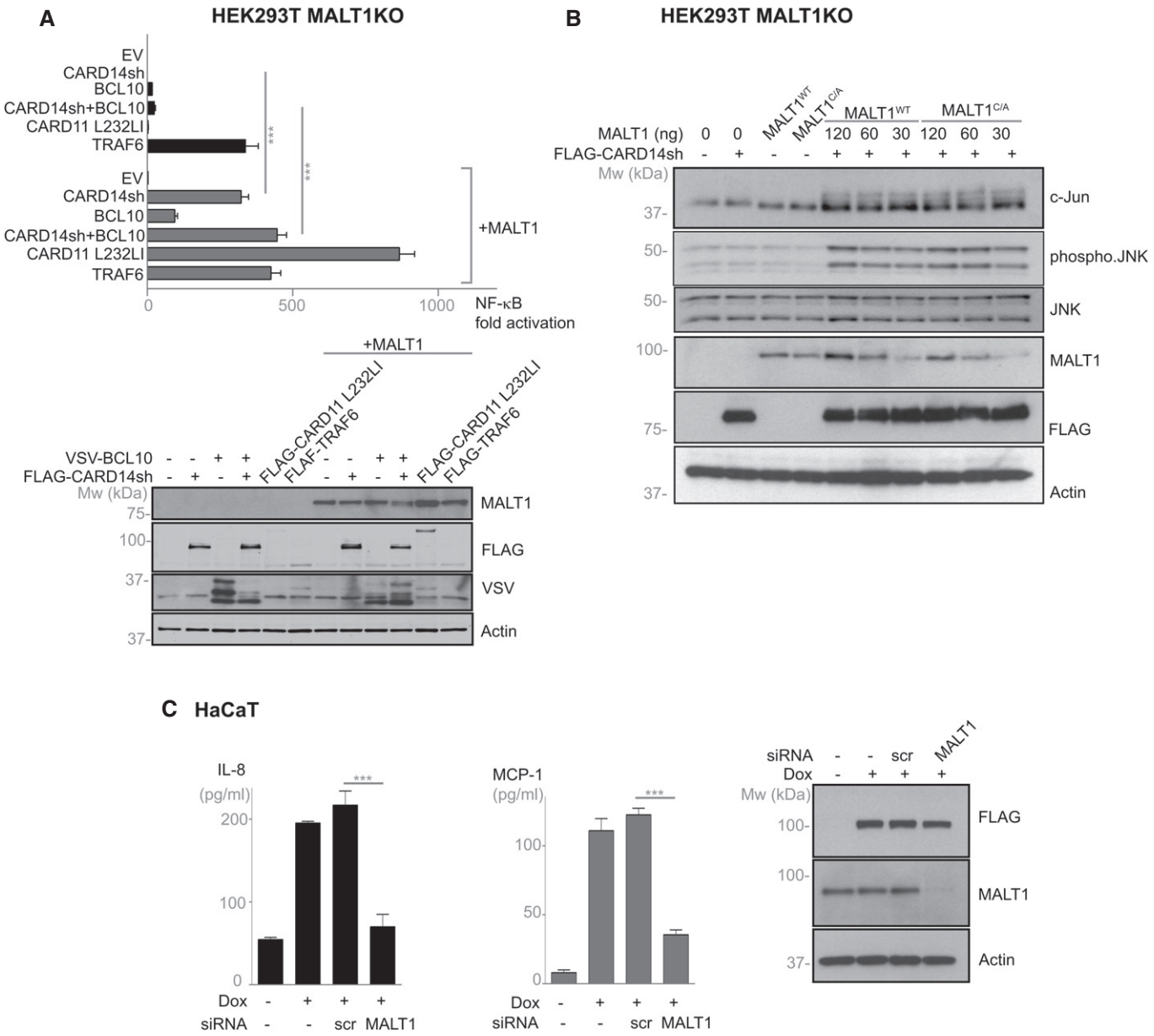

Figure 3. MALT1 deficiency prevents CARD14sh-induced NF-κB/JNK signaling and inflammatory gene expression.

A MALT1 expression is essential for CARD14sh-induced NF-κB activation. MALT1-deficient HEK293T cells were transfected with NF-κB reporter plasmid and the indicated expression plasmids. Luciferase activity in cell lysates was measured 24 h later. CARD11(L232LI) and TRAF6 transfections were used as MALT1-dependent and MALT1-independent controls, respectively. Expression of the transfected plasmids was verified by immunoblotting (lower panel).

B MALT1 expression is essential for CARD14sh-induced JNK activation. MALT1-deficient HEK293T cells were transfected with FLAG-CARD14sh (30 ng) either alone or together with either wild-type ($MALT1^{WT}$) or catalytically inactive MALT1 ($MALT1^{C/A}$) as indicated. c-Jun accumulation and JNK phosphorylation were analyzed by immunoblotting with the antibodies indicated. Actin was used as a loading control.

C MALT1 deficiency inhibits CARD14-induced gene expression in HaCaT keratinocytes. HaCaT cells were transfected with scrambled (scr) or MALT1-targeting siRNA prior to doxycycline-induced CARD14 expression as described in Materials and Methods. IL-8 and MCP-1 concentration in the cell supernatants was measured 8 h (IL-8) or 24 h (MCP-1) later by ELISA. Doxycycline-induced CARD14 expression and MALT1 knockdown were verified by immunoblotting (right panel). Data are representative of two independent experiments.

Data information: Values are the mean of triplicates ± SE. Significance levels: ***$P < 0.001$ by Student's *t*-test.

For all CARD14 variants, MALT1 knockdown strongly reduced IL-8 production (Fig 6C). We repeatedly observed a small decrease in basal IL-8 production upon MALT1 siRNA transfection (also reflected in the lower signal in cells stimulated with TNF, which is MALT1-independent). This may reflect a cellular stress response due to MALT1 knockdown, or a role for an endogenous protein that is induced upon siRNA transfection and which induces IL-8 expression in a MALT1-dependent manner. Finally, inhibition of MALT1

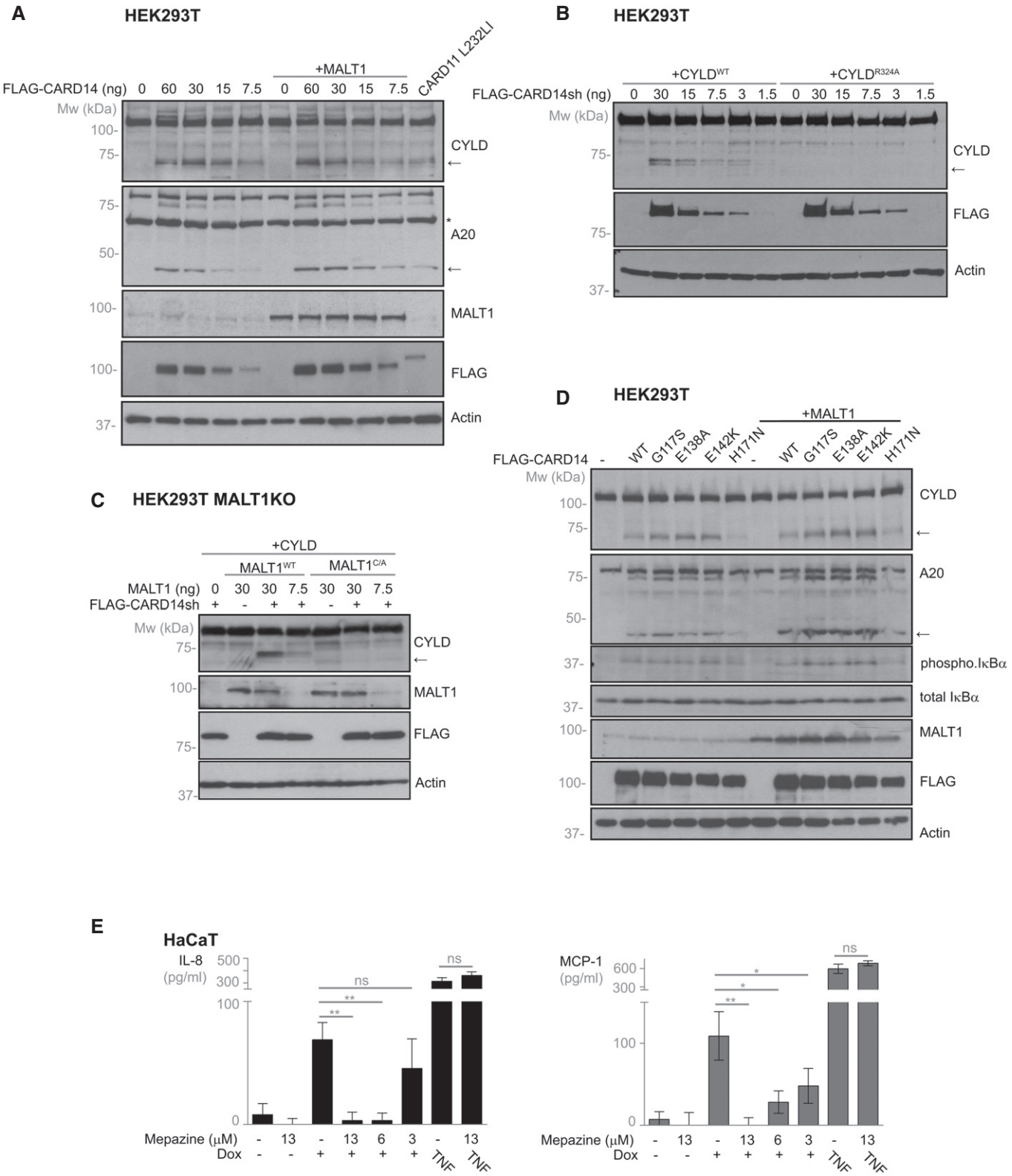

Figure 4.

proteolytic activity by mepazine also drastically diminished IL-8 induction by the different CARD14 variants in primary human keratinocytes, whereas TNF-induced IL-8 production was unaffected (Fig 6D, upper panel). As expected, CARD14-induced A20 cleavage, which was most pronounced in the case of CARD14(E138A), was also inhibited by mepazine treatment (Fig 6D, lower panel). The

Figure 4. CARD14 signaling activates MALT1 proteolytic activity.

A CARD14 signaling induces CYLD and A20 cleavage. HEK293T cells were transfected with different concentrations of FLAG-CARD14, with or without MALT1 as indicated. CARD11(L232LI) transfection was used as a positive control. Endogenous CYLD and A20 processing was analyzed by immunoblotting. CYLD and A20 cleavage fragments are indicated by an arrow, the asterisk indicates a non-specific band.

B CARD14 signaling induces CYLD cleavage after R324. HEK293T cells were transfected with different concentrations of FLAG-CARD14sh and either wild-type ($CYLD^{WT}$) or non-cleavable CYLD ($CYLD^{R324A}$). CYLD processing was analyzed by immunoblotting. The CYLD cleavage fragment is indicated by an arrow.

C Expression of catalytically active MALT1 is necessary for CARD14-induced CYLD cleavage. MALT1-deficient HEK293T cells, in which MALT1 expression was restored by transfection with different concentrations of either wild-type ($MALT1^{WT}$) or catalytically inactive MALT1 ($MALT1^{C/A}$), were co-transfected with FLAG-CARD14sh and CYLD as indicated. CYLD processing was analyzed by immunoblotting. The CYLD cleavage fragment is indicated by an arrow.

D Psoriasis-associated CARD14 mutation enhances activation of MALT1 proteolytic activity. HEK293T cells were transfected with wild-type (WT) FLAG-CARD14 or different psoriasis-associated CARD14 mutants (20 ng), with or without MALT1 (20 ng) as indicated. Endogenous CYLD and A20 processing, as well as IκBα phosphorylation, was analyzed by immunoblotting. The CYLD and A20 cleavage fragments are indicated by an arrow.

E Pharmacological inhibition of MALT1 proteolytic activity prevents CARD14-induced gene expression in HaCaT keratinocytes. CARD14 expression was induced by doxycycline (dox) treatment in the absence or presence of different concentrations of mepazine as indicated. The next morning, cell culture medium was refreshed and IL-8 and MCP-1 concentration in the cell supernatant was measured 8 h later by ELISA. TNF stimulation (MALT1-independent) was used as a negative control. Values are the mean of triplicates ± SE. Data are representative of two independent experiments. Significance levels: $*P < 0.05$, $**P < 0.001$ by Student's *t*-test.

Source data are available online for this figure.

apparently slight increase in A20 cleavage observed upon TNF stimulation can be explained by a TNF-induced increase in A20 expression, leading to a higher basal A20 cleavage. Collectively, our data demonstrate a hitherto unknown role of MALT1 in wild-type and psoriasis-associated mutant CARD14-mediated inflammatory signaling in human primary keratinocytes.

Discussion

In the present study, we demonstrate a key role for paracaspase MALT1 in CARD14-induced signaling. We confirm previous analyses that CARD14 activates NF-κB and extend this by also showing effects on p38/JNK signaling, both of which are shown to depend on the presence of MALT1. Of note, the related protein CARD11 also mediates TCR-induced NF-κB and JNK signaling, but is not essential for p38 MAP kinase activation [35]. In addition, we show that CARD14 expression induces the formation of a novel CBM complex and MALT1 proteolytic activity. The physiological relevance for psoriasis is illustrated by our finding that the enhanced ability of psoriasis-associated CARD14 mutants to activate NF-κB relative to wild-type CARD14 is more pronounced when MALT1 is co-expressed. We show that pathogenic CARD14 mutants more efficiently activate MALT1 proteolytic activity, which is associated with enhanced BCL10/MALT1 binding. Moreover, we show that mutant CARD14-induced cytokine and chemokine expression in human primary keratinocytes can be strongly decreased by MALT1 deficiency or a MALT1 protease inhibitor, providing evidence that MALT1 might be a valuable therapeutic target in psoriasis associated with CARD14 mutation.

Because stimuli or receptors that activate CARD14-mediated signaling have not yet been identified, we were limited to the use of CARD14 overexpression to activate downstream signaling. It was previously shown that cells express multiple splice variants of CARD14, with a shorter variant known as CARD14sh being the most abundant [4,12]. CARD14sh still encodes the N-terminal CARD and coiled-coil domains that are sufficient for NF-κB activation as well as a PDZ domain, but lacks the SH3 and GUK domains. Most published studies only used CARD14sh. Here, we show that overexpression of full-length CARD14 induces NF-κB-dependent gene expression as well as p38/JNK activation with largely similar efficiency as CARD14sh, excluding an important role for the SH3 and GUK domains. In other proteins, these domains are known to mediate important protein–protein interactions [36]. We cannot exclude that these domains still play a role at endogenous expression levels or in other still to identify CARD14-induced signaling pathways. Consistent with previous findings made with psoriasis-associated CARD14sh mutants [3,4], overexpression of full-length CARD14 (G117S), CARD14(E138A), and CARD14(E142K) induced NF-κB activation more potently than wild-type CARD14. These mutations are located in the linker region between the CARD and coiled-coil domain or in the beginning of the coiled-coil domain itself. Most likely the amino acid substitutions cause some conformational changes in CARD14 that affect intra- or intermolecular interactions

Figure 5. CARD14sh-induced NF-κB signaling is negatively regulated by CYLD, A20, and ABIN1.

A, B CYLD and A20 inhibit CARD14sh-induced NF-κB activation. HEK293T cells were transfected with NF-κB reporter plasmid and FLAG-tagged CARD14sh (30 ng), with or without the indicated concentrations of CYLD (A) or A20 (B). Luciferase activity in cell lysates was measured 24 h later. Protein expression of transfected plasmids was verified by Western blot and is shown in the accompanying panels. Closed arrowheads indicate full-length A20 and CYLD; arrows indicate cleaved A20 and CYLD. Data are representative of three independent experiments.

C A20 and ABIN-1 inhibit CARD14-induced NF-κB activation. HEK293T cells were transfected with NF-κB reporter plasmid, A20 (3 ng) or ABIN1 (15 ng) and the indicated concentrations of FLAG-tagged CARD14sh. Luciferase activity in cell lysates was measured 24 h later. Protein expression of transfected plasmids was verified by Western blot and is shown in the accompanying panels. Data are representative of three independent experiments.

D A20 inhibits CARD14-induced NF-κB activation through its ZnF domains. HEK293T cells were transfected with NF-κB reporter plasmid, FLAG-CARD14sh (20 ng) and wild-type (WT) or mutant A20 expression plasmids (3 ng) as indicated. Luciferase activity in cell lysates was measured after 24 h. CARD14 and A20 expression was measured by immunoblotting (right panel). Data are representative of two independent experiments.

Data information: Values are the mean of triplicates ± SE. Significance levels: ns $P > 0.05$, $*P < 0.05$, $**P < 0.001$, $***P < 0.001$ by Student's *t*-test. In panel (D), *P*-values are compared against the "CARD14-only" set-up.

that are important for NF-κB signaling. This hypothesis is further supported by our observation that relative to wild-type CARD14, CARD14(E138A) shows enhanced interaction with MALT1.

We showed that CARD14 is part of a novel CARD14–BCL10–MALT1 (CBM) signaling complex. This resembles the CBM complexes that are formed by CARD9, CARD10 and CARD11 in

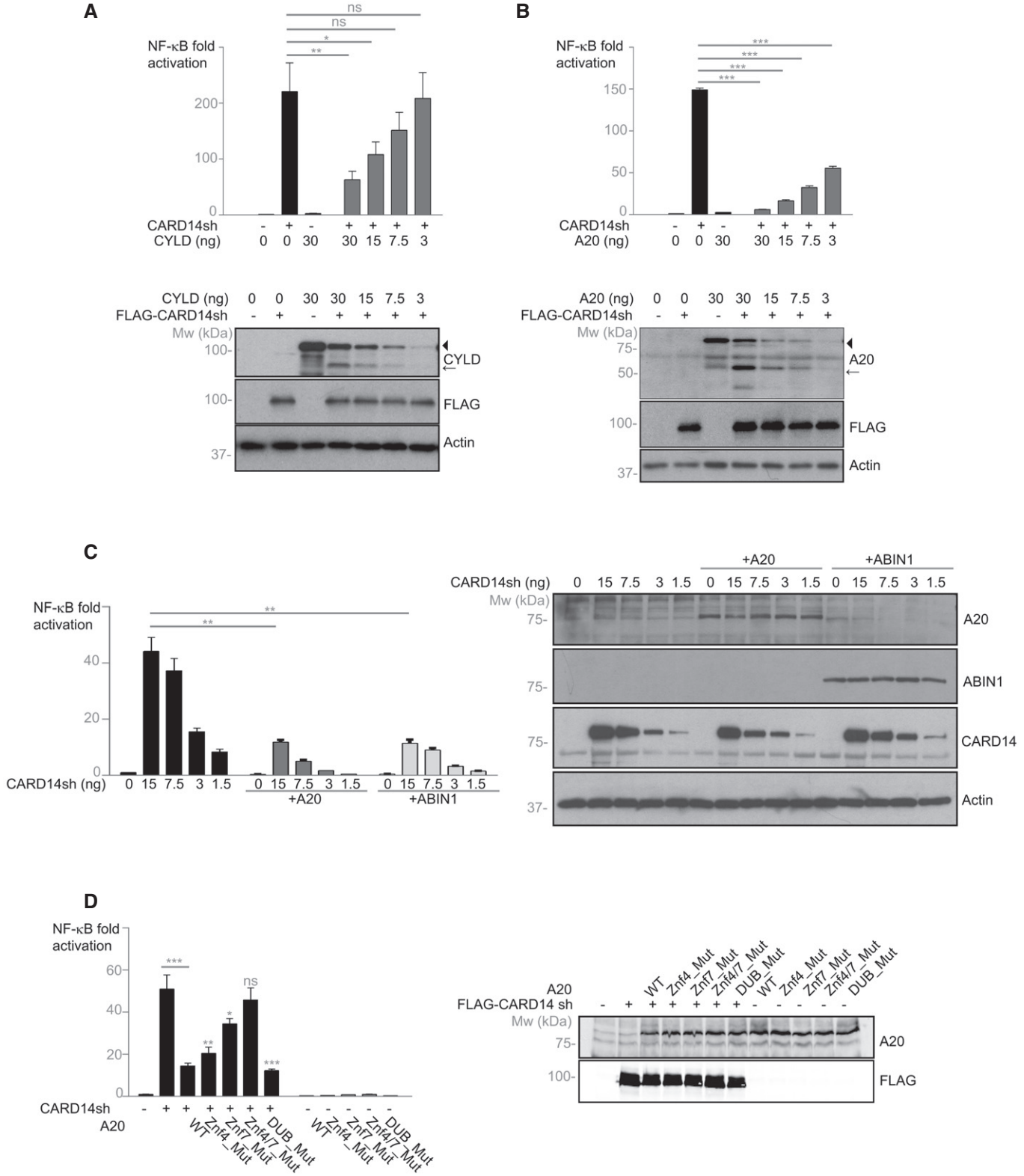

Figure 5.

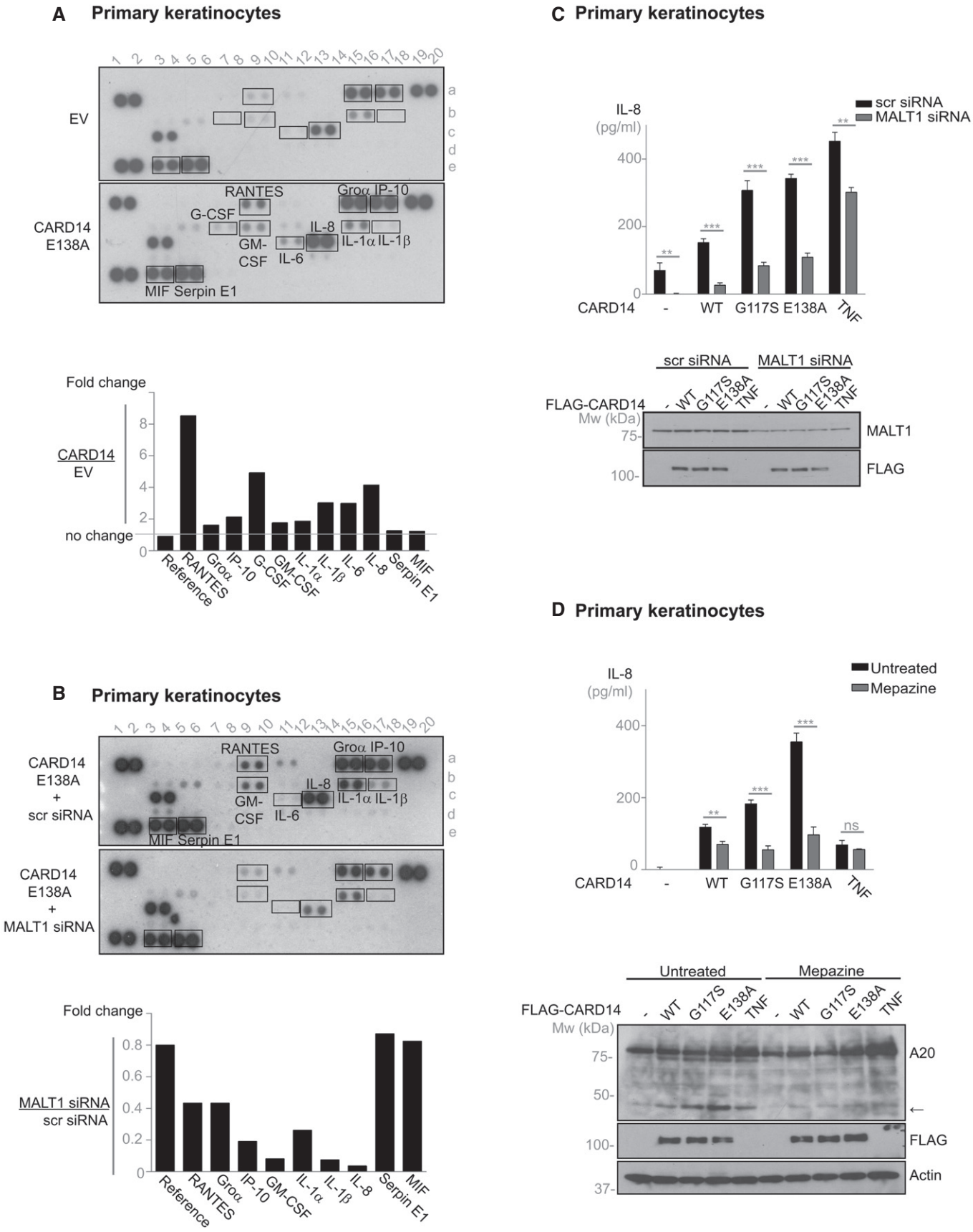
A Primary keratinocytes
EV
CARD14 E138A
RANTES
Groα IP-10
G-CSF
IL-8
GM-CSF
IL-6
IL-1α IL-1β
MIF Serpin E1
Fold change
CARD14 EV
no change
Reference
RANTES
Groα IP-10
G-CSF
GM-CSF
IL-1α
IL-1β
IL-6
IL-8
Serpin E1
MIF
B Primary keratinocytes
CARD14 E138A + scr siRNA
CARD14 E138A + MALT1 siRNA
MALT1 siRNA scr siRNA
C Primary keratinocytes
IL-8 (pg/ml)
scr siRNA
MALT1 siRNA
CARD14 - WT G117S E138A TNF
FLAG-CARD14
Mw (kDa)
MALT1
FLAG
D Primary keratinocytes
Untreated
Mepazine
ns
A20
Actin

Figure 6.

Figure 6. Pathogenic mutant CARD14-induced gene expression and A20 cleavage in human primary keratinocytes is MALT1-dependent.

A CARD14(E138A) induces cytokine and chemokine expression in human primary keratinocytes. Cells were transfected with empty vector (EV) or CARD14(E138A) as indicated. Twenty-four hours later, the secretion of 36 different human cytokines, chemokines, and acute-phase proteins was analyzed via a multiplex antibody array. Quantification was done using ImageJ software and is expressed as relative CARD14/EV values for a selected number of proteins (bottom panel).

B MALT1 deficiency inhibits CARD14(E138A)-induced cytokine and chemokine expression in human primary keratinocytes. Cells were transfected with scrambled (scr) or MALT1-targeting siRNA as indicated, 48 h later followed by transfection with CARD14(E138A). After 24 h, cytokine and chemokine expression was analyzed and is expressed as described in (A).

C Pathogenic CARD14 mutation enhances MALT1-dependent CARD14-induced IL-8 expression in human primary keratinocytes. Cells were transfected with scrambled (scr) or MALT1-targeting siRNA as indicated, 48 h later followed by transfection with CARD14 wild-type (WT), CARD14(G117S), or CARD14(E138A) as indicated. TNF treatment was used as a control. After 24 h, IL-8 concentration in the cell supernatant was analyzed via ELISA. Expression levels of MALT1 and CARD14 variants were verified by immunoblotting (bottom panel).

D Pharmacological inhibition of MALT1 proteolytic activity inhibits CARD14-induced IL-8 production and A20 processing in human primary keratinocytes. Cells were transfected with different CARD14 variants in the presence or absence of mepazine as indicated. TNF treatment was used as a control. Twenty-four hours later, IL-8 levels in the cell supernatant were measured by ELISA. Expression of different CARD14 variants and CARD14-induced processing of endogenous A20 were analyzed by immunoblotting. A20 cleavage fragment is indicated by an arrow. Data are representative of two independent experiments.

Data information: Values are the mean of triplicates ± SE. Significance levels: ns $P > 0.05$, $^{**}P < 0.001$, $^{***}P < 0.001$ by Student's *t*-test.
Source data are available online for this figure.

response to dectin-1, GPCR, and T-cell receptor stimulation, respectively [7]. CBM complex formation was equally efficient for CARD14 and CARD14sh, excluding an important role for the C-terminal MAGUK signature of CARD14. A MAGUK signature is also absent in CARD9, whose ability to form a CBM complex was, however, found to be much less efficient than CARD14sh. These data suggest that structural differences between CARD9 (absence of a complete MAGUK signature) and CARD14sh (still having the protein and lipid interacting PDZ part of the MAGUK signature) might provide unique regulatory mechanisms.

Our observation that CARD14-induced NF-κB signaling and JNK signaling are fully compromised in MALT1-deficient cells reveals a key role for MALT1 in CARD14 signaling. Most importantly, we showed that CARD14 expression also activates the proteolytic activity of MALT1, resulting in the cleavage of known MALT1 substrates such as A20 and CYLD. Overexpression of A20 and CYLD diminished CARD14-induced NF-κB signaling, suggesting that CARD14 activity is under the control of A20 and CYLD. This is especially interesting since, besides *CARD14*, single nucleotide polymorphisms in *A20* and *CYLD* have been associated with psoriasis susceptibility [24–27]. Because the psoriasis-associated SNPs in these genes are located outside the coding region, possibly regulating A20 and CYLD expression, we could not determine the effect of the corresponding mutations on NF-κB signaling induced by CARD14sh overexpression.

Mechanistically, it has been suggested that in lymphocytes MALT1 protease activity controls the prolonged DNA-binding capacity of only a subset of RelA- and c-Rel-containing NF-κB complexes via degradation of the NF-κB family member RelB [37]. In addition, MALT1 has recently been shown to regulate the stability of specific mRNAs in lymphocytes by cleaving the RNA binding proteins Regnase-1 and Roquin [22,23]. It is therefore likely that MALT1 uses similar mechanisms in keratinocytes to control the expression of a subset of genes. This is further suggested by our observation that pharmacological inhibition of MALT1 proteolytic activity significantly inhibits the CARD14-induced expression of IL-8 and MCP-1 in keratinocytes. If and how CARD14-induced cleavage of A20, CYLD, or other proteins contributes to this finding remains to be investigated.

Because of its essential role in the activation and proliferation of lymphocytes, selective inhibition of MALT1 protease activity holds significant potential for the treatment of autoimmune disease. This is supported by the fact that MALT1 small-molecule inhibitors are protective in a mouse model for multiple sclerosis [38]. Moreover, inhibition of MALT1 proteolytic activity is selectively toxic to human lymphoma cell lines that exhibit aberrant MALT1 activity *in vitro* and xenotransplanted tumors *in vivo* [39,40]. Therapeutic inhibition of CARD11/MALT1-mediated T-cell activation is also relevant in the context of psoriasis and other inflammatory skin diseases. Our finding that CARD14 activates MALT1 proteolytic activity and inflammatory gene expression in keratinocytes, which are enhanced by psoriasis-associated mutations of *CARD14*, suggests an additional contribution of MALT1 activation in keratinocytes to the pathology of psoriasis. While this manuscript was under revision, MALT1 activity was also shown to control zymosan-induced expression of inflammatory genes in keratinocytes [41], which further supports our findings. Moreover, we show that MALT1 inhibitor treatment prevents mutant CARD14-induced expression of several psoriasis-associated cytokines and chemokines in human primary keratinocytes, which can be expected to affect keratinocyte–immune cell interactions. Future studies testing the effect of genetic inactivation of MALT1 in keratinocytes versus T cells or other cell types combined with murine models of psoriasis will be very informative. Recently, some concern has been raised on the concept of chronic and systemic inhibition of MALT1 because knock-in mice expressing catalytically inactive MALT1 develop multi-organ inflammation due to the absence of regulatory T-cell development [42–45] (and reviewed in [10]), although it remains to be seen whether therapeutic targeting of MALT1 in adult mice would suffer from similar toxicity. In addition, in the context of psoriasis topical treatment with MALT1 inhibitors can be expected to induce less side effects than systemic inhibition of MALT1 activity. Although more challenging to develop, molecules that specifically target the interaction of mutant CARD14 with BCL10/MALT1 may allow to specifically interfere with pathological MALT1 activation in keratinocytes and be the most safe approach to treat psoriasis patients with CARD14 mutations.

Materials and Methods

Antibodies

The following antibodies were used: anti-FLAG M2 monoclonal antibody (A-8592, Sigma, St Louis, MO, USA), anti-myc monoclonal

antibody produced in-house, anti-VSV-G polyclonal antibody (V4888, Sigma, St Louis, MO, USA), anti-MALT1 polyclonal antibody (sc-28246, Santa Cruz, Heidelberg, Germany or ab33921, Abcam, Cambridge, UK), anti-CARD14 polyclonal antibody (HPA023388, Sigma), anti-c-Jun polyclonal antibody (sc-1694, Santa Cruz), anti-phospho-c-Jun (Ser63) polyclonal antibody (#9261, Cell Signaling Technology, MA, USA), anti-JNK1/2 phosphospecific polyclonal antibody (446826G, Invitrogen, NY, USA), anti-JNK1/2 monoclonal antibody (554285, BD Biosciences, CA, USA), anti-p38 MAPK polyclonal antibody (#9212, Cell Signaling Technology), anti-phospho-p38 MAPK (Thr180/Tyr182) monoclonal antibody (#9215, Cell Signaling Technology), anti-IκBα polyclonal antibody (sc-371, Santa Cruz), anti-phospho-IκBα (Ser32/36) (#9246, Cell Signaling Technology), anti-actin monoclonal antibody (MP6472J, MP Biomedicals, Illkirch Cedex, France), anti-CYLD monoclonal antibody (sc-74435, Santa Cruz), anti-A20 monoclonal antibody (sc-52910 or sc-166692, Santa Cruz), anti-ABIN1 monoclonal antibody (37-6100, Invitrogen), anti-p44/42MAPK (Erk1/2) polyclonal antibody (#9102, Cell Signaling Technology), and anti-phospho-p44/42 MAPK (Erk1/2) (Thr202/Tyr204) polyclonal antibody (#9101, Cell Signaling Technology). Secondary HRP-conjugated anti-mouse or anti-rabbit IgG antibody was purchased from Amersham (Diegem, Belgium).

Expression plasmids

pNFconluc (LMBP3248), which contains NF-κB-driven luciferase, was a gift from Dr. A. Israël (Institut Pasteur, Paris, France); pACTβgal (LMBP4341) was from Dr. J. Inoue (Institute of Medical Sciences, Tokyo, Japan), pReceiver-M11-Flag-CARD14sh was a gift from Prof. A. Bowcock (Imperial College, London, UK). The following plasmids are available at the BCCM-LMBP plasmid collection (http://bccm.belspo.be/about-us/bccm-lmbp) along with detailed sequence maps: pCD-MALT1 (LMBP05536), pCD-MALT1(C464A) (LMBP05541), pRC3-hBCL10 (LMBP06967), pCD-BCL10 (LMBP05535), pCD-CARD11(L232LI) (mouse) (LMBP07889), pCAGGS-CYLD (LMBP06613), pCAGGS-CYLD(R324A) (LMBP06645), pCAGGS-hA20 (LMBP03778), pME-TRAF6 (LMBP06043), pCAGGS-hABIN-1 (LMBP07130), pCDNA3-hCARD9 (LMBP09609), pCAGGS-hA20 (LMBP03778), pCAGGS-hA20(C624A–C627A) (ZF4_Mut; LMBP06563), pCAGGS-hA20(C775A–C779A) (ZF7_Mut; LMBP06569), pCAGGS-hA20 (C624A–C627A/C775A–C779A) (ZF4/7_Mut; LMBP06570), and pCAGGS-hA20(D100A/C103A) (DUB_Mut; LMBP06056). Full-length CARD14 was amplified from HeLa S3 cDNA using following forward 5′-ATGGGGGAACTGTGCCG-3′ and reverse 5′-TCATCGGGGGCTCTG CT-3′ primers. The PCR product was cloned into EcoRV-opened pCDNA3 or pCDNA3.1-FLAG vector and verified by sequencing. Full-length CARD14 psoriasis-associated mutants G117S, E138A, E142K, and H171N were generated by PCR mutagenesis.

Cells, plasmid transfection, and siRNA-mediated knockdown

HEK293T (gift from Dr. M. Hall; Department of Biochemistry, University of Birmingham, UK) and HaCaT cells (immortalized human keratinocytes) were cultured in Dulbecco's modified Eagle's medium, supplemented with 10% fetal calf serum and 2 mM L-glutamine. MALT1-deficient HEK293T cells were generated using TALEN-mediated gene targeting. Briefly, HEK293T were seeded at 10^5 per well in a 6-well plates and transfected with 1 μg of MALT1 TALEN plasmid pair (H43180, TALEN Library Resource, Seoul, Korea) on two consecutive days. Cells were serially diluted and clones lacking MALT1 expression were selected by immunoblotting. For transfection, HEK293T cells were seeded at 4×10^4 cells/well in 24-well plates and transiently transfected by the calcium phosphate precipitation method. BCL10 was knocked down in HEK293T cells with BCL10-specific siRNA smartpool (Dharmacon) using Lipofectamine RNAiMax (Invitrogen); non-targeting siRNA pool was used as a control.

HaCaT cells harboring a dox-inducible *CARD14* gene were generated using retroviral transduction. Briefly, full-length CARD14 was subcloned into pDG2lenti_Flag rtTA3 puro (LMBP7944) lentiviral vector. Viral particles were produced in HEK293T cells (3×10^6 cells per 75-cm^2 flask) transfected with 10 μg CARD14-lentivector along with VSV-G and packaging plasmids. Cells were washed 6 h later, and 7 ml of fresh media was added to the flask. Supernatant containing viral particles was collected 48 h after transfection and filtered through a 0.45-μm filter. Two milliliters of the supernatant supplemented with 8 μg/ml polybrene was applied to HaCaT cells seeded at 10^5 cells per well of a 6-well plates. Infection was repeated 6 h later for additional 18 h. Cells were expanded and selected by addition of puromycin (1.5 μg/ml). Expression of CARD14 was induced by the addition of 1 μg/ml doxycycline (Sigma) and confirmed by immunoblotting. In knockdown experiments, HaCaT cells were seeded at 2×10^5 cells per well in 6-well plates. Twenty-four hours and 48 h later, cells were transfected with 5 pmol of non-targeting or MALT1-specific siRNA smartpool (Dharmacon) using Lipofectamine RNAiMAX (Invitrogen). Six hours later, cells were trypsinized and seeded in Opti-MEM (Life Technologies, Belgium) at 4×10^4 cells per well in 24-well plates in the presence or absence of 1 μg/ml of doxycycline to induce CARD14 expression. Media were exchanged the next day for fresh OptiMEM, and cells were left for additional 8 h or 24 h, after which supernatants were collected for IL-8 (eBioscience, CA, USA) and MCP-1 (BD Biosciences) measurement by ELISA.

Primary human keratinocytes were purchased from Cell Systems (FC-0007, Troisdorf, Germany) and cultured in Dermalife-K (LM-0027, Cell Systems, Germany). For transfection, 2.5×10^4 cells were seeded in 24-well plates and 24 h later transiently transfected using PromoFectin (PromoKine, Heidelberg, Germany). INTERFERin® (Polyplus Transfection, France) was used for reverse transfection of 4×10^4 cells with 10 nM of non-targeting or MALT1-specific siRNA smartpool (Dharmacon). Forty-eight hours later, the cells were transfected with plasmid DNA as described. Twenty-four hours after transfection, cell supernatants were collected and cytokine levels were measured by ELISA or human cytokine array (ProteomeProfiler®, R&D Systems, UK) according to the manufacturer's protocol.

All cells used were free of mycoplasma as measured via the PlasmoTest Mycoplasma detection kit (InvivoGen, San Diego, USA).

NF-κB-dependent reporter assay

Twenty-four hours after transfection, HEK293T cells were lysed in 200 μl luciferase lysis buffer (25 mM Tris-phosphate pH 7.8, 2 mM dithiothreitol, 2 mM 1,2-cyclohexaminediaminetetraacetic acid, 10% glycerol, and 1% Triton X-100), followed by luciferase and β-galactosidase activity measurements. Luciferase values were

normalized by β-galactosidase values in order to correct for potential differences in transfection efficiency.

Co-immunoprecipitation

HEK293T cells were seeded at 1×10^6 cells on 90-mm Petri dishes and transfected with a total of 5 μg DNA. Twenty-four hours later, cells were lysed in MALT1 IP buffer (20 mM Tris–HCl pH 7.5, 137 mM NaCl, 1.5 mM $MgCl_2$, and 1% Triton X-100) supplemented with protease and phosphatase inhibitors. Cell extracts were pre-cleared with 1 μg of total rabbit IgG (sc-2027, Santa Cruz) and 15 μl protein G-Sepharose beads (GE Healthcare, Buckinghamshire, UK). Proteins were precipitated with 1 μg of anti-MALT1 antibody (Abcam) for 2 h at 4°C followed by the addition of 15 μl protein G-Sepharose beads for 1 h. The beads were washed four times with 1 ml lysis buffer and resuspended in 40 μl Laemmli buffer. Proteins were separated by SDS–PAGE and analyzed by Western blotting.

Statistical analysis

Results are expressed as mean ± SE. Differences between two groups were assessed using multiple two-tailed Student's *t*-tests and corrected for multiple comparisons via the Holm–Sidak method. Statistical calculations were performed using Prism 6 software (GraphPad Software Inc.).

Expanded View for this article is available online.

Acknowledgements
Research in the authors' laboratory is supported by grants from the "Fund for Scientific Research Flanders (FWO)"; "Belgian Foundation Against Cancer"; "Agency for Innovation by Science and Technology (IWT)"; "Interuniversity Attraction Poles"; Ghent University ("Hercules", "Concerted Research Actions (GOA)", "Group-ID Multidisciplinary research partnership") and a European Commission granted TOLLerant H2020-MSC-ETN-642157 project. E.V.N. and I.A. are supported by a predoctoral and postdoctoral fellowship, respectively, from the FWO.

Author contributions
ISA, EVN, JS, and RB conceived and designed the experiments. IAS, EVN, GB, YD, and MK performed the experiments. IAS, EVN, and RB analyzed the data, interpreted the results, and wrote the manuscript.

Conflict of interest
The authors declare that they have no conflict of interest.

References

1. Lowes MA, Suarez-Farinas M, Krueger JG (2014) Immunology of psoriasis. *Annu Rev Immunol* 32: 227 – 255
2. Albanesi C, De Pita O, Girolomoni G (2007) Resident skin cells in psoriasis: a special look at the pathogenetic functions of keratinocytes. *Clin Dermatol* 25: 581 – 588
3. Jordan CT, Cao L, Roberson ED, Duan S, Helms CA, Nair RP, Duffin KC, Stuart PE, Goldgar D, Hayashi G *et al* (2012) Rare and common variants in CARD14, encoding an epidermal regulator of NF-kappaB, in psoriasis. *Am J Hum Genet* 90: 796 – 808
4. Jordan CT, Cao L, Roberson ED, Pierson KC, Yang CF, Joyce CE, Ryan C, Duan S, Helms CA, Liu Y *et al* (2012) PSORS2 is due to mutations in CARD14. *Am J Hum Genet* 90: 784 – 795
5. Fuchs-Telem D, Sarig O, van Steensel MA, Isakov O, Israeli S, Nousbeck J, Richard K, Winnepenninckx V, Vernooij M, Shomron N *et al* (2012) Familial pityriasis rubra pilaris is caused by mutations in CARD14. *Am J Hum Genet* 91: 163 – 170
6. Berki DM, Liu L, Choon SE, David Burden A, Griffiths CE, Navarini AA, Tan ES, Irvine AD, Ranki A, Ogo T *et al* (2015) Activating CARD14 mutations are associated with generalized pustular psoriasis but rarely account for familial recurrence in psoriasis vulgaris. *J Invest Dermatol* 135: 2964 – 2970
7. Blonska M, Lin X (2011) NF-kappaB signaling pathways regulated by CARMA family of scaffold proteins. *Cell Res* 21: 55 – 70
8. Scudiero I, Vito P, Stilo R (2014) The three CARMA sisters: so different, so similar: a portrait of the three CARMA proteins and their involvement in human disorders. *J Cell Physiol* 229: 990 – 997
9. Hulpiau P, Driege Y, Staal J, Beyaert R (2016) MALT1 is not alone after all: identification of novel paracaspases. *Cell Mol Life Sci* 73: 1103 – 1116
10. Demeyer A, Staal J, Beyaert R (2016) Targeting MALT1 proteolytic activity in immunity, inflammation and disease: good or bad? *Trends Mol Med* 22: 135 – 150
11. Hailfinger S, Lenz G, Thome M (2014) Targeting B-cell lymphomas with inhibitors of the MALT1 paracaspase. *Curr Opin Chem Biol* 23C: 47 – 55
12. Scudiero I, Zotti T, Ferravante A, Vessichelli M, Vito P, Stilo R (2011) Alternative splicing of CARMA2/CARD14 transcripts generates protein variants with differential effect on NF-kappaB activation and endoplasmic reticulum stress-induced cell death. *J Cell Physiol* 226: 3121 – 3131
13. Bertin J, Wang L, Guo Y, Jacobson MD, Poyet JL, Srinivasula SM, Merriam S, DiStefano PS, Alnemri ES (2001) CARD11 and CARD14 are novel caspase recruitment domain (CARD)/membrane-associated guanylate kinase (MAGUK) family members that interact with BCL10 and activate NF-kappa B. *J Biol Chem* 276: 11877 – 11882
14. Johansen C, Kragballe K, Westergaard M, Henningsen J, Kristiansen K, Iversen L (2005) The mitogen-activated protein kinases p38 and ERK1/2 are increased in lesional psoriatic skin. *Br J Dermatol* 152: 37 – 42
15. Takahashi H, Ibe M, Nakamura S, Ishida-Yamamoto A, Hashimoto Y, Iizuka H (2002) Extracellular regulated kinase and c-Jun N-terminal kinase are activated in psoriatic involved epidermis. *J Dermatol Sci* 30: 94 – 99
16. Ip YT, Davis RJ (1998) Signal transduction by the c-Jun N-terminal kinase (JNK)–from inflammation to development. *Curr Opin Cell Biol* 10: 205 – 219
17. Gross O, Gewies A, Finger K, Schafer M, Sparwasser T, Peschel C, Forster I, Ruland J (2006) Card9 controls a non-TLR signalling pathway for innate anti-fungal immunity. *Nature* 442: 651 – 656
18. Bertin J, Guo Y, Wang L, Srinivasula SM, Jacobson MD, Poyet JL, Merriam S, Du MQ, Dyer MJ, Robison KE *et al* (2000) CARD9 is a novel caspase recruitment domain-containing protein that interacts with BCL10/CLAP and activates NF-kappa B. *J Biol Chem* 275: 41082 – 41086
19. Baens M, Bonsignore L, Somers R, Vanderheydt C, Weeks SD, Gunnarsson J, Nilsson E, Roth RG, Thome M, Marynen P (2014) MALT1 auto-proteolysis is essential for NF-kappaB-dependent gene transcription in activated lymphocytes. *PLoS ONE* 9: e103774
20. Coornaert B, Baens M, Heyninck K, Bekaert T, Haegman M, Staal J, Sun L, Chen ZJ, Marynen P, Beyaert R (2008) T cell antigen receptor stimulation induces MALT1 paracaspase-mediated cleavage of the NF-kappaB inhibitor A20. *Nat Immunol* 9: 263 – 271

21. Staal J, Driege Y, Bekaert T, Demeyer A, Muyllaert D, Van Damme P, Gevaert K, Beyaert R (2011) T-cell receptor-induced JNK activation requires proteolytic inactivation of CYLD by MALT1. *EMBO J* 30: 1742 – 1752
22. Jeltsch KM, Hu D, Brenner S, Zoller J, Heinz GA, Nagel D, Vogel KU, Rehage N, Warth SC, Edelmann SL *et al* (2014) Cleavage of roquin and regnase-1 by the paracaspase MALT1 releases their cooperatively repressed targets to promote T(H)17 differentiation. *Nat Immunol* 15: 1079 – 1089
23. Uehata T, Iwasaki H, Vandenbon A, Matsushita K, Hernandez-Cuellar E, Kuniyoshi K, Satoh T, Mino T, Suzuki Y, Standley DM *et al* (2013) Malt1-induced cleavage of regnase-1 in CD4(+) helper T cells regulates immune activation. *Cell* 153: 1036 – 1049
24. Nair RP, Duffin KC, Helms C, Ding J, Stuart PE, Goldgar D, Gudjonsson JE, Li Y, Tejasvi T, Feng BJ *et al* (2009) Genome-wide scan reveals association of psoriasis with IL-23 and NF-kappaB pathways. *Nat Genet* 41: 199 – 204
25. Tejasvi T, Stuart PE, Chandran V, Voorhees JJ, Gladman DD, Rahman P, Elder JT, Nair RP (2012) TNFAIP3 gene polymorphisms are associated with response to TNF blockade in psoriasis. *J Invest Dermatol* 132: 593 – 600
26. Oudot T, Lesueur F, Guedj M, de Cid R, McGinn S, Heath S, Foglio M, Prum B, Lathrop M, Prud'homme JF *et al* (2009) An association study of 22 candidate genes in psoriasis families reveals shared genetic factors with other autoimmune and skin disorders. *J Invest Dermatol* 129: 2637 – 2645
27. Nititham J, Taylor KE, Gupta R, Chen H, Ahn R, Liu J, Seielstad M, Ma A, Bowcock AM, Criswell LA *et al* (2015) Meta-analysis of the TNFAIP3 region in psoriasis reveals a risk haplotype that is distinct from other autoimmune diseases. *Genes Immun* 16: 120 – 126
28. Verstrepen L, Carpentier I, Verhelst K, Beyaert R (2009) ABINs: A20 binding inhibitors of NF-kappa B and apoptosis signaling. *Biochem Pharmacol* 78: 105 – 114
29. Sun SC (2010) CYLD: a tumor suppressor deubiquitinase regulating NF-kappaB activation and diverse biological processes. *Cell Death Differ* 17: 25 – 34
30. Catrysse L, Vereecke L, Beyaert R, van Loo G (2014) A20 in inflammation and autoimmunity. *Trends Immunol* 35: 22 – 31
31. De A, Dainichi T, Rathinam CV, Ghosh S (2014) The deubiquitinase activity of A20 is dispensable for NF-kappaB signaling. *EMBO Rep* 15: 775 – 783
32. Verhelst K, Carpentier I, Kreike M, Meloni L, Verstrepen L, Kensche T, Dikic I, Beyaert R (2012) A20 inhibits LUBAC-mediated NF-kappaB activation by binding linear polyubiquitin chains via its zinc finger 7. *EMBO J* 31: 3845 – 3855
33. Fukuoka M, Ogino Y, Sato H, Ohta T, Komoriya K, Nishioka K, Katayama I (1998) RANTES expression in psoriatic skin, and regulation of RANTES and IL-8 production in cultured epidermal keratinocytes by active vitamin D3 (tacalcitol). *Br J Dermatol* 138: 63 – 70
34. Chiricozzi A, Guttman-Yassky E, Suarez-Farinas M, Nograles KE, Tian S, Cardinale I, Chimenti S, Krueger JG (2011) Integrative responses to IL-17 and TNF-alpha in human keratinocytes account for key inflammatory pathogenic circuits in psoriasis. *J Invest Dermatol* 131: 677 – 687
35. Hara H, Wada T, Bakal C, Kozieradzki I, Suzuki S, Suzuki N, Nghiem M, Griffiths EK, Krawczyk C, Bauer B *et al* (2003) The MAGUK family protein CARD11 is essential for lymphocyte activation. *Immunity* 18: 763 – 775
36. Gonzalez-Mariscal L, Betanzos A, Avila-Flores A (2000) MAGUK proteins: structure and role in the tight junction. *Semin Cell Dev Biol* 11: 315 – 324
37. Hailfinger S, Nogai H, Pelzer C, Jaworski M, Cabalzar K, Charton JE, Guzzardi M, Decaillet C, Grau M, Dorken B *et al* (2011) Malt1-dependent RelB cleavage promotes canonical NF-kappaB activation in lymphocytes and lymphoma cell lines. *Proc Natl Acad Sci USA* 108: 14596 – 14601
38. Mc Guire C, Elton L, Wieghofer P, Staal J, Voet S, Demeyer A, Nagel D, Krappmann D, Prinz M, Beyaert R *et al* (2014) Pharmacological inhibition of MALT1 protease activity protects mice in a mouse model of multiple sclerosis. *J Neuroinflammation* 11: 124
39. Nagel D, Spranger S, Vincendeau M, Grau M, Raffegerst S, Kloo B, Hlahla D, Neuenschwander M, Peter von Kries J, Hadian K *et al* (2012) Pharmacologic inhibition of MALT1 protease by phenothiazines as a therapeutic approach for the treatment of aggressive ABC-DLBCL. *Cancer Cell* 22: 825 – 837
40. Fontan L, Yang C, Kabaleeswaran V, Volpon L, Osborne MJ, Beltran E, Garcia M, Cerchietti L, Shaknovich R, Yang SN *et al* (2012) MALT1 small molecule inhibitors specifically suppress ABC-DLBCL in vitro and in vivo. *Cancer Cell* 22: 812 – 824
41. Schmitt A, Grondona P, Maier T, Brandle M, Schonfeld C, Jager G, Kosnopfel C, Eberle FC, Schittek B, Schulze-Osthoff K *et al* (2016) MALT1 protease activity controls the expression of inflammatory genes in keratinocytes upon zymosan stimulation. *J Invest Dermatol* 136: 788 – 797
42. Gewies A, Gorka O, Bergmann H, Pechloff K, Petermann F, Jeltsch KM, Rudelius M, Kriegsmann M, Weichert W, Horsch M *et al* (2014) Uncoupling malt1 threshold function from paracaspase activity results in destructive autoimmune inflammation. *Cell Rep* 9: 1292 – 1305
43. Jaworski M, Marsland BJ, Gehrig J, Held W, Favre S, Luther SA, Perroud M, Golshayan D, Gaide O, Thome M (2014) Malt1 protease inactivation efficiently dampens immune responses but causes spontaneous autoimmunity. *EMBO J* 33: 2765 – 2781
44. Bornancin F, Renner F, Touil R, Sic H, Kolb Y, Touil-Allaoui I, Rush JS, Smith PA, Bigaud M, Junker-Walker U *et al* (2015) Deficiency of MALT1 paracaspase activity results in unbalanced regulatory and effector T and B cell responses leading to multiorgan inflammation. *J Immunol* 194: 3723 – 3734
45. Yu JW, Hoffman S, Beal AM, Dykon A, Ringenberg MA, Hughes AC, Dare L, Anderson AD, Finger J, Kasparcova V *et al* (2015) MALT1 protease activity is required for innate and adaptive immune responses. *PLoS ONE* 10: e0127083